Available online at www.sciencedirect.com
ScienceDirect
Trans. Nonferrous Met. Soc. China 22(2012) 842−846
Transactions of Nonferrous Metals Society of China
www.tnmsc.cn

Effects of Y addition on structural and mechanical properties of CuZrAl bulk metallic glass

XU Hong-wei[1, 2], DU Yu-lei[1, 2], DENG Yu[3]

1. Engineering Research Center of Materials Behavior and Design of Ministry of Education,
School of Materials Science and Engineering, Nanjing University of Science and Technology, Nanjing 210094, China;
2. Jiangsu Institute of Advanced Materials, Danyang 212300, China;
3. National Laboratory of Solid State Microstructures, Center for Materials Analysis,
Nanjing University, Nanjing 210093, China

Received 9 September 2011; accepted 12 January 2012

Abstract: The effects of Y addition on the structural and mechanical properties of CuZrAl bulk metallic glass (BMG) were studied. The results show that the glass forming ability of CuZrAl system is improved by the addition of Y and the fracture strength decreases with Y addition due to the reduction of binding energy induced by Y. The fracture surface is dominated by vein-like patterns in $Cu_{45}Zr_{48}Al_7$ bulk metallic glass, and changes to smooth regions in $Cu_{46}Zr_{42}Al_7Y_5$ BMG. TEM observation shows that $Cu_{45}Zr_{48}Al_7$ BMG has a composite microstructure of nanocrystalline phases dispersed in amorphous matrix. However, the $Cu_{46}Zr_{42}Al_7Y_5$ BMG shows a fully amorphous structure.

Key words: bulk metallic glass; Cu-based alloy; Y addition

1 Introduction

Bulk metallic glasses (BMGs) are considered new structural materials due to their unique mechanical, physical and chemical properties [1−5]. It is reported that the glass forming ability (GFA), physical, chemical and mechanical properties of BMGs can be greatly affected by the addition of rare earth metals [6, 7]. For example, it is found that the GFA of Fe-, Zr- and Ti-based BMGs can be enhanced by minor addition of Y [8−10]. The reason for the improvement is that the addition of Y can restrain the formation of crystalline phases and scavenge oxygen from the undercooled liquid [11]. Recently, the excellent enhancement in GFA by the addition of Y has been also found in Cu-based BMGs [12]. As reported, the fully amorphous $Cu_{46}Zr_{47-x}Al_7Y_x$ ($0\le x\le 10$) BMGs with diameter from 4 up to 10 mm could be easily prepared by an injection mold casting.

Compared to Zr-, Pd-, Fe- and Ti-based BMGs [1,2, 13−15], Cu-based BMGs with high GFA are more promising for industrial applications because of their relatively low cost and no toxic element like Be or Ni [16−20]. To promote their applications, the combination of high GFA and excellent mechanical properties of Cu-based BMGs is expected. However, in the previous work, it was found that the fracture strength of a Zr-based BMG decreased with increasing Y content [21]. Up to now, the effects of Y on the mechanical properties of Cu-based BMGs have not been clearly clarified. Therefore, it is valuable to reveal the effects of Y on the structural and mechanical properties of CuZrAl BMGs. In the present work, $Cu_{45}Zr_{48}Al_7$ and $Cu_{46}Zr_{42}Al_7Y_5$ BMGs were prepared. The effects of Y on the GFA, thermal stability and fracture strength were studied. The difference in the fracture surface and local-order microstructure induced by Y was also studied by SEM and HRTEM.

2 Experimental

The alloy ingots of $Cu_{45}Zr_{48}Al_7$ and $Cu_{46}Zr_{42}Al_7Y_5$ were prepared by arc melting the mixtures of Cu, Zr, Al and Y metals in a Ti-gettered argon atmosphere. All

Foundation item: Project (2010ZDJH10) supported by the NUST Research Funding; Project (BK2007213) supported by the Natural Science Foundation of Jiangsu Province, China
Corresponding author: DU Yu-lei; Tel: +86-25-84315159; Fax: +86-25-84315159; E-mail: yldu_njust@mail.njust.edu.cn
DOI: 10.1016/S1003-6326(11)61254-5

elements used are of >99.95% purity. Each ingot was melted at least five times to ensure the homogeneity. The alloy ingots were remelted in a fused glass tube under a vacuum level of about 5×10^{-3} Pa and then injection cast with ultrahigh purity argon into a copper mold to prepare cylindrical rods with size of *d*3 mm×100 mm. X-ray diffraction (XRD) with Cu K_α radiation for phase identification was performed on the as-cast samples via θ−2θ scans. The thermal stability of the as-cast samples was examined by differential scanning calorimetry (DSC) at a constant heating rate of 20 K/min in argon atmosphere using a Netzsch STA 449C device. Room temperature compression tests were carried out with a WDW−200D machine under a maximum load of 200 kN at an engineering strain rate of 5×10^{-4} s^{-1}. The cross-sectional surfaces of the $Cu_{45}Zr_{48}Al_7$ and $Cu_{46}Zr_{42}Al_7Y_5$ samples were examined using a S−3400N II scanning electron microscope (SEM). Specimens for transmission electron microscopy (TEM) were prepared by standard twin-jet electrolytic thinning with a HNO_3−CH_3OH electrolyte (volume ratio of 7:3). The microstructure was observed by TEM on a JEM−200CX instrument.

3 Results and discussion

Figure 1 shows the XRD patterns of the as-cast $Cu_{45}Zr_{48}Al_7$ and $Cu_{46}Zr_{42}Al_7Y_5$ alloys. It can be seen that the patterns of the two alloys exhibit only a broad diffraction maximum without any observable crystalline peaks, demonstrating the formation of a fully amorphous structure.

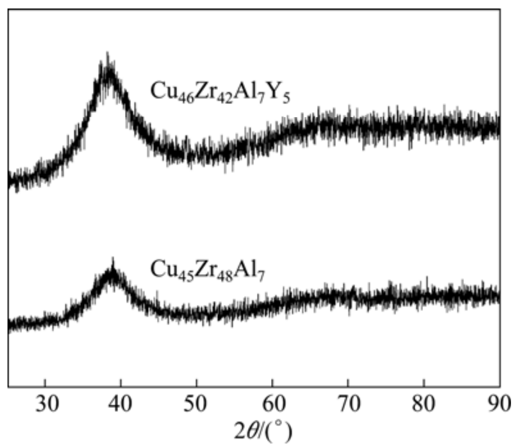

Fig. 1 XRD patterns of as-cast $Cu_{45}Zr_{48}Al_7$ and $Cu_{46}Zr_{42}Al_7Y_5$ alloys

The DSC curves of the as-cast $Cu_{45}Zr_{48}Al_7$ and $Cu_{46}Zr_{42}Al_7Y_5$ samples are shown in Fig. 2. During heating, both of the samples exhibit a distinct endothermic peak due to glass transition, followed by a supercooled liquid region, and then a sharp exothermic peak due to crystallization. The glass transition temperature (T_g) and the onset temperature of crystallization (T_x) are measured to be 700 and 761 K, 678 and 759 K for $Cu_{45}Zr_{48}Al_7$ and $Cu_{46}Zr_{42}Al_7Y_5$ alloys, respectively. The corresponding supercooled liquid region $\Delta T(T_x-T_g)$ are calculated to be 61 and 81 K, respectively. Obviously, the addition of Y expands the supercooled liquid region, indicating the improvement of the glass forming ability of CuZrAl bulk metallic glass. As shown in Fig. 2, the exothermic peaks tend to be broadened with Y addition, indicating a possible slow-down in the kinetics of crystal nucleation and growth. It is known that the glass forming ability can be strongly affected by the large negative heat of mixing among the constituent elements. The mixture heat of Y−Cu, Y−Al and Zr−Cu are −22, −31 and −23 kJ/mol, respectively [22]. Therefore, the formation of an inhomogeneous structure, such as short- or medium-range ordering clusters in the amorphous phase can be hindered by the addition of Y in CuZrAl system, which leads to the improvement of the glass forming ability of CuZrAl BMGs.

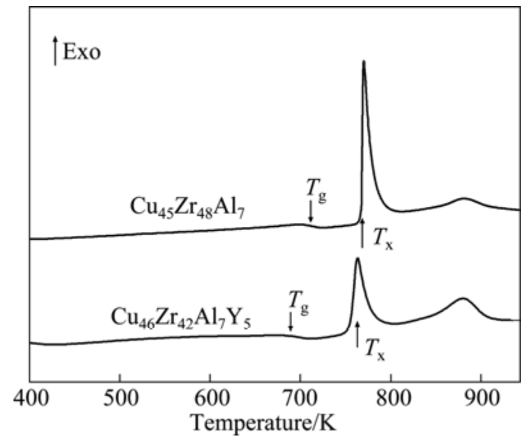

Fig. 2 DSC curves of as-cast $Cu_{45}Zr_{48}Al_7$ and $Cu_{46}Zr_{42}Al_7Y_5$ rods at heating rate of 20 K/min

Figure 3 illustrates the room temperature compressive engineering stress—strain curves of the as-cast $Cu_{45}Zr_{48}Al_7$ and $Cu_{46}Zr_{42}Al_7Y_5$ rods with dimensions of *d*3 mm×6 mm. As can be seen, both of the two samples exhibit brittle fracture without any macroscopic plastic deformation. It is seen that the ductility of CuZrAl BMGs is not improved by the addition of Y. The compressive fracture strength of $Cu_{45}Zr_{48}Al_7$ and $Cu_{46}Zr_{48}Al_7Y_5$ samples is measured to be about 1892 and 1465 MPa, respectively. Obviously, the strength of the CuZrAl bulk metallic glass decreases with the addition of Y. In previous work, a drop in ultimate fracture strength induced by the addition of Y was also found in a Zr-based bulk metallic glass. As known, the ultimate fracture strength of BMGs is related to the binding energy of constituent elements [23]. For BMGs, the binding energy is proportional to the glass transition temperature [24]. That is, the higher T_g is, the higher the binding energy is. As shown in Fig. 2, the value of T_g decreases greatly with the addition of Y. Thus, the decrease in the fracture strength of $Cu_{46}Zr_{42}Al_7Y_5$ BMG can be ascribed to the decrease of the binding energy induced by Y addition.

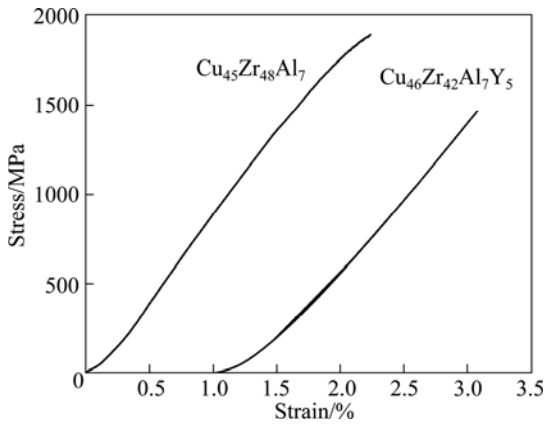

Fig. 3 Engineering stress—strain curves of $Cu_{45}Zr_{48}Al_7$ and $Cu_{46}Zr_{42}Al_7Y_5$ bulk metallic glasses under room temperature compression

Figure 4 shows the compressive fracture surface of $Cu_{45}Zr_{48}Al_7$ and $Cu_{46}Zr_{42}Al_7Y_5$ BMGs. It can be seen that the fracture surface is dominated by typical vein-like patterns, which indicates that local softening takes place. In addition, some intermittent smooth regions are also observed on the surface. However, as shown in Fig. 4(b), the fracture surface of $Cu_{46}Zr_{42}Al_7Y_5$ BMG is characterized by smooth featureless regions with larger spaced striations on the surface, which form during the fast crack propagation. Generally, the fracture surface of BMGs contains vein-like patterns, river-like patterns and smooth regions. The vein-like patterns are indicative of the ductile fracture in BMGs [25,26]. Based on the changes in the fracture morphology induced by Y, it can be concluded that the $Cu_{46}Zr_{42}Al_7Y_5$ BMG is more brittle than $Cu_{45}Zr_{48}Al_7$ BMG, which is also supported by the fact that the samples of $Cu_{46}Zr_{42}Al_7Y_5$ BMG shatter into dozens of pieces when compressed.

To understand the different brittle fracture behavior of $Cu_{45}Zr_{48}Al_7$ and $Cu_{46}Zr_{42}Al_7Y_5$ BMGs, TEM observation was carried out to reveal the difference in their microstructures. Figure 5(a) shows the HRTEM image of the $Cu_{45}Zr_{48}Al_7$ BMG exhibiting the microstructure of nanometer-sized crystalline phase embedded in the amorphous matrix. Moreover, the selected-area diffraction electron pattern (inset in Fig. 5(a)) presents strong diffraction spots on the background of halo rings, indicating a composite microstructure of nanocrystalline phases dispersed in

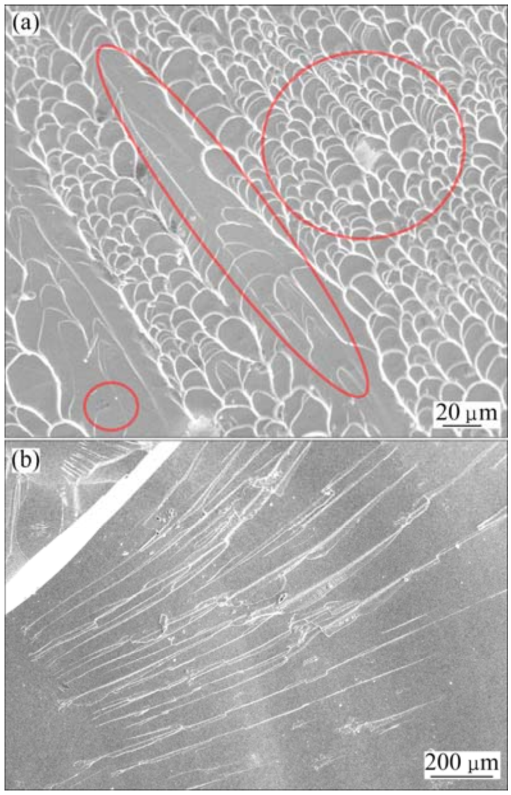

Fig. 4 SEM images of compressive fracture surface of $Cu_{45}Zr_{48}Al_7$ (a) and $Cu_{46}Zr_{42}Al_7Y_5$ (b) BMGs

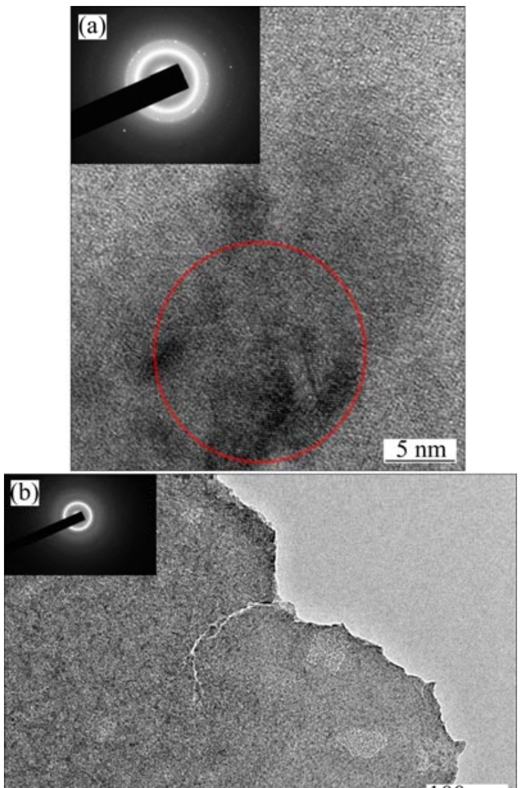

Fig. 5 HRTEM images of $Cu_{45}Zr_{48}Al_7$ (a) and $Cu_{46}Zr_{42}Al_7Y_5$ (b) BMGs and corresponding selected-area electron diffraction patterns

amorphous matrix. However, the TEM image of $Cu_{46}Zr_{42}Al_7Y_5$ BMG demonstrates a uniform amorphous structure within the resolution of the TEM adopted, as shown in Fig. 5(b). The corresponding selected-area electron diffraction inserted in Fig. 5(b) presents only halo diffraction intensity, which further supports the fully amorphous structure of $Cu_{46}Zr_{42}Al_7Y_5$ BMG. From the differences in microstructure of $Cu_{45}Zr_{48}Al_7$ and $Cu_{46}Zr_{42}Al_7Y_5$ BMGs, it can be concluded that the formation of nanometer-sized clusters in CuZrAl BMGs is hindered by the addition of Y, which leads to the improvement of GFA and the formation of fully amorphous structure. The more brittle nature of $Cu_{46}Zr_{42}Al_7Y_5$ BMGs may be related to the fully amorphous structure.

4 Conclusions

1) $Cu_{45}Zr_{48}Al_7$ and $Cu_{46}Zr_{42}Al_7Y_5$ bulk metallic glasses are prepared by copper mold melting method. Compared to $Cu_{45}Zr_{48}Al_7$ bulk metallic glass, the T_g of $Cu_{46}Zr_{42}Al_7Y_5$ BMGs decreases and the supercooled liquid region widens, indicating the improvement of GFA due to Y addition.

2) The fracture strength decreases after Y addition due to the reduction in binding energy. The fracture surface is dominated by vein-like patterns in $Cu_{45}Zr_{48}Al_7$ BMG, however, it changes to smooth regions in $Cu_{46}Zr_{42}Al_7Y_5$ BMGs, indicating $Cu_{46}Zr_{42}Al_7Y_5$ BMG is more brittle than Y-free $Cu_{45}Zr_{48}Al_7$ BMG.

3) The TEM results show that $Cu_{45}Zr_{48}Al_7$ BMG has a composite microstructure of nanocrystalline phases dispersed in amorphous matrix. However, the $Cu_{46}Zr_{42}Al_7Y_5$ BMG exhibits a fully amorphous structure. It is suggested that the improvement in GFA and decrease of mechanical properties induced by Y addition in CuZrAl-based BMGs should be carefully balanced.

References

[1] INOUE A. Stabilization of metallic supercooled liquid and bulk amorphous alloys [J]. Acta Mater, 2000, 48(1): 279−306.

[2] SCHUH C A, HUFNAGEL T C, RAMAMURTY U. Mechanical behavior of amorphous alloys [J]. Acta Mater, 2007, 55(12): 4067−4109.

[3] WU Y, XIAO Y H, CHEN G L, LIU C T, LU Z P. Bulk metallic glass composites with transformation mediated work-hardening and ductility [J]. Adv Mater, 2010, 22(25): 2770−2773.

[4] LIU L, QIU C L, CHEN Q, ZHANG S M. Corrosion behavior of Zr-based bulk metallic glasses in different artificial body fluids [J]. J Alloys Compd, 2006, 425(1−2): 268−273.

[5] CORNELISON S G, ZHAO J G, SELLMYER D J. Rare earth gallium iron glasses (II): Anomalous magnetic hysteresis in alloys based on Pr, Nd and Sm [J]. Phys Rev B, 1984, 30(5): 2857−2865.

[6] MATTERN N, VAINIO U, PARK J M, HAN J H, SHARIQ A, KIM D H, ECKERT J. Phase separation in $Cu_{46}Zr_{47-x}Al_7Gd_x$ metallic glasses [J]. J Alloys Compd, 2010, 509(S1): s23−s26.

[7] ZHANG Y, CHEN J, CHEN G L, LIU X J. Glass formation mechanism of minor yttrium addition in CuZrAl alloys [J]. Appl Phys Lett, 2006, 89(13): 131904-1−3.

[8] LU Z P, LIU C T, THOMPSON J R, PORTER W D. Structural amorphous steels [J]. Phys Rev Lett, 2004, 92(24): 245503-1−4.

[9] LU Z P, LIU C T, PORTER W D. Role of yttrium in glass formation of Fe-based bulk metallic glasses [J]. Appl Phys Lett, 2003, 83(13): 2581−2584.

[10] HAO G J, REN F, ZHANG Y, LIN J P. Role of yttrium in glass formation of Ti-based bulk metallic glasses [J]. Rare Metals, 2009, 28(1): 68−71.

[11] LU Z P, LIU C T. Glass formation criterion for various glass-forming systems [J]. Phys Rev Lett, 2003, 91(11): 115505-1−4.

[12] XU H, DUAN G, JOHNSON W L. Unusual glass-forming ability of bulk amorphous alloys based on ordinary metal copper [J]. Phys Rev Lett, 2007, 92(24): 245504-1−4.

[13] SUN G Y, CHEN G, CHEN G L. Comparison of microstructures and properties of Zr-based bulk metallic glss composites with dendritic and spherical bcc phase precipitates [J]. Intermetallics, 2007, 15(5−6): 632−634.

[14] CHENG J L, CHEN G, XU F, DU Y L, LI Y S, LIU C T. Correlation of the microstructure and mechanical properties of Zr-based in-situ bulk metallic glass matrix composites [J]. Intermetallics, 2010, 18(12): 2425−2430.

[15] SUN G Y, CHEN G, LIU C T, CHEN G L. Innovative processing and property improvement of metallic glass based composites [J]. Scripta Materialia, 2006, 55: 375−378.

[16] INOUE A, ZHANG W, ZHANG T, KUROSAKA K. High-strength Cu-based bulk glassy alloy in Cu−Zr−Ti and Cu−Hf−Ti ternary systems [J]. Appl Phys Lett, 2001, 49(14): 2645−2652.

[17] LOUZGUINE D V, KATO H, INOUE A. High-strength Cu-based crystal-glassy composite with enhanced ductility [J]. Appl Phys Lett, 2004, 84(7): 1088.

[18] PAULY S, DAS J, BEDNARCIK J, MATTERN N, KIM K B, KIM D H, ECKERT J. Deformation induced martensitic transformation in Cu−Zr−(Al, Ti) bulk metallic glass composites [J]. Scripta Mater, 2009, 60(6): 431−434.

[19] KOVACS Z S, REVESZ A. Effect of local ordering on the decomposition of an amorphous CuZrTi alloy [J]. Appl Phys Lett, 2005, 87(25): 251909-1−3.

[20] SUN B A, YU H B, JIAO W, BAI H Y, ZHAO D Q, WANG W H. Plasticity of ductile metallic glasses: A self-organized critical state [J]. Phys Rev Lett, 2010, 105(3): 035501-1−4.

[21] YAN M, ZOU J, SHEN J. Effect of over-doped yttrium on the microstructure, mechanical properties and thermal properties of a Zr-based metallic glass [J]. Acta Mater, 2006, 54(13): 3627−3635.

[22] TAKEUCHI A, INOUE A. Classification of bulk metallic glasses by atomic size difference, heat of mixing and period of constituent elements and its application to characterization of the main alloying element [J]. Mater Trans, 2005, 46(12): 2817−2829.

[23] LI J, NGAN A H W, GUMBSCH P. Atomistic modeling of mechanical behavior [J]. Acta Mater, 2003, 51(19): 5711−5742.

[24] CHEN H S. Metallic glasses [J]. Mater Sci Eng, 1976, 25: 59−69.

[25] ZHANG Z F, ECKERT J, SCHULTZ L. Difference in compressive and tensile fracture mechanisms of $Zr_{59}Cu_{20}Al_{10}Ni_8Ti_3$ bulk metallic glass [J]. Acta Mater, 2003, 51(4): 1167−1179.

[26] PAN J, LIU L, CHAN K C. Enhanced plasticity by phase separation in CuZrAl bulk metallic glass with micro-addition of Fe [J]. Scripta Mater, 2009, 60(9): 822−825.

Y 元素添加对 CuZrAl 块体金属玻璃的结构和力学性能的影响

许宏伟[1,2]，杜宇雷[1,2]，邓　昱[3]

1. 南京理工大学 材料评价与设计教育部工程研究中心，南京 210094；
2. 江苏省(丹阳)高性能合金材料研究院，丹阳 212300；
3. 南京大学 固态微结构国家重点实验室，现代分析中心，南京 210093

摘　要：研究添加 Y 元素对 CuZrAl 块体金属玻璃的结构和力学性能的影响。结果表明，添加 Y 元素提高 CuZrAl 体系的玻璃形成能力，而且由于添加 Y 元素可以降低该体系的结合能，从而降低其断裂强度。$Cu_{45}Zr_{48}Al_7$ 块体金属玻璃的断裂表面主要呈脉状，而 $Cu_{46}Zr_{42}Al_7Y_5$ 块体金属玻璃的断裂表面则很平滑。TEM 观察表明，$Cu_{45}Zr_{48}Al_7$ 的微观结构为非晶基体中含有纳米相，然而 $Cu_{46}Zr_{42}Al_7Y_5$ 块体金属玻璃为全非晶结构。

关键词：块体金属玻璃；Cu 基合金；Y 添加

(Edited by FANG Jing-hua)